Fermilab FERMILAB-CONF-07-263-AD June 2007

MODELING AND DESIGN OF THE ILC TEST AREA BEAM ABSORBERS AT FERMILAB*

M.D. Church, A.Z. Chen, N.V. Mokhov, S. Nagaitsev, N. Nakao
Fermilab, Bavia, IL 60510, USA

July 16, 2007

Abstract

Detailed MARS15 simulations have been performed on energy deposition and shielding of the proposed ILC Test Area absorbers. It is designed for up to 50 kW of 800-MeV electron beam power and provides unlimited occupancy conditions in the experimental hall. ANSYS analysis based on the calculated energy deposition maps confirms robustness of the proposed design of the absorbers and beam windows for normal operation and for various failure modes.

*Presented paper at the *2007 Particle Accelerator Conference (PAC07)*, Albuquerque, NM, June 25-29, 2007

MODELING AND DESIGN OF THE ILC TEST AREA BEAM ABSORBERS AT FERMILAB *

M.D. Church, A.Z. Chen, N.V. Mokhov, S. Nagaitsev, N. Nakao†, Fermilab, Batavia, IL 60510, USA

Abstract

Detailed MARS15 simulations have been performed on energy deposition and shielding of the proposed ILC Test Area absorbers. It is designed for up to 50 kW of 800-MeV electron beam power and provides unlimited occupancy conditions in the experimental hall. ANSYS analysis based on the calculated energy deposition maps confirms robustness of the proposed design of the absorbers and beam windows for normal operation and for various failure modes.

INTRODUCTION

Fermilab ILC Test Area (ILCTA) beam dumps and their shielding have been designed based on simulations with the MARS15 [1] code. A main dump after a third cryomodule is absorbing a 800-MeV electron beam. It is placed at the end of a hall below a loading dock. The beam is assumed to be 2×10^{10} electrons per bunch, with 3000 bunches and 1-ms trains at 5 Hz, i.e. about 50 μA.

Initially, the beam RMS spot size on the dump has been assumed to be σ_x=σ_y = 3 mm. The dump is designed to handle up to 50 kW of the beam power at 800 MeV. The beam dump will be in atmosphere.

BEAM DUMP CORE DESIGN

A graphite core encapsulated in a water-cooled aluminum core-box is an obvious choice for the dump. This is an extremely robust design proven, e.g., by 27 years of operation of the Tevatron beam dump [2], and used at many accelerator facilities around the world. The ILCTA beam parameters are very similar to those of the TESLA Test Facility (TTF), therefore it is not a surprise that the core parameters found in MARS15 simulations (Fig. 1) are similar to those of the TTF: 20×20×90 cm graphite core in a water-cooled aluminum core-box 15-cm thick transversely and 35-cm downstream of the core, followed by a 50×50×60 cm copper absorber.

THERMAL AND STRESS ANALYSIS

Beam Dump

Beam-induced power density profiles simulated by MARS15 are shown in Fig. 2. The peak power density in graphite is about 120 W/g for the full beam. Although with a good cooling system this should not be a problem, it is desirable to increase the beam σ on the dump by about a factor of two. The total power of up to 50 kW should be removed from the core by water flowing either in pipes on the outside of the aluminum core-box or in the groves as in the Tevatron dump [2]. With the dimensions chosen and appropriate cooling, heating in aluminum, copper absorber and surrounding shielding is quite acceptable.

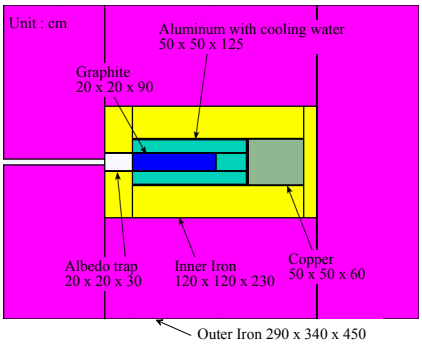

Figure 1: Beam dump materials and dimensions as chosen in MARS optimization calculations.

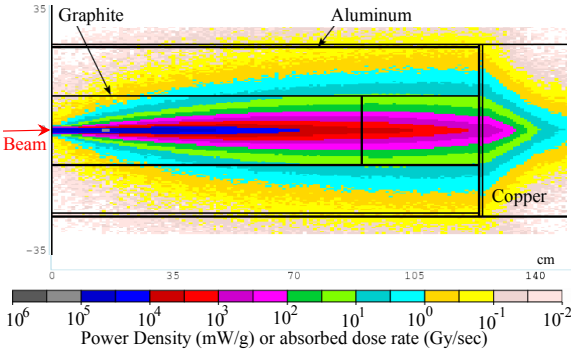

Figure 2: Power density isocontours in the dump core.

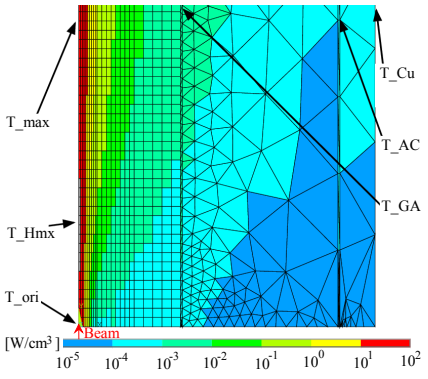

Figure 3: Dump model of 2D axis-symmetry for ANSYS.

* Work supported by Fermi Research Alliance, LLC, under contract No. DE-AC02-07CH11359 with the U.S. Department of Energy.

† nakao@fnal.gov

Table 1: Parameters used in ANSYS simulation

	T °C	Material Al	Graph	Cu	Be	Ti
Thermal Conductivity (W/cm/K)	27	2.40	1.14	3.85	2.16	0.10
	127	2.40	0.92			
	327	2.30	0.75			
	527	2.20	0.70			
	727	0.93	0.55			
Specific Heat (J/g/K)	27	0.858	0.568	0.39	1.93	0.57
	127	0.951	0.994			
	327	1.037	1.409			
	527	1.177	1.779			
	727	1.177	2.089			
Density (g/cm^3)		2.70	1.71	0.86	1.85	4.6
Thermal Expansion Rates (10^{-6}/K)		25.8	6.7	17.0	12.6	8.5
Ultimate Strength (MPa)					565	685
Yield Strength (MPa)					538	560

In order to study characteristics of heating in the dump core, ANSYS thermal calculation was performed with a 2D azimuthally symmetric model using the power density distribution in the dump core shown in Fig. 2 as a heating source. Fig.3 shows the 2D model of the simulation with graphite core, aluminum layer and copper layer. Water cooling (with convection coefficient of 10000 [W/m^2/K] at 30 °C) was applied on the outer surface of aluminum. Natural air cooling (5 [W/m^2/K] at 25 °C) was on the outer surfaces of copper and the front surfaces. The non-perfect thermal contact on the interfaces between different materials was treated as a thin layer with a reduced thermal conductivity. The parameters used are given in Table 1.

Fig.4 shows temperature rises from static state (thermal equilibrium state) as water cooling accidentally failed at the 6 interesting locations in the first 10000 second. From the ANSYS study above, the following conclusions can be made:

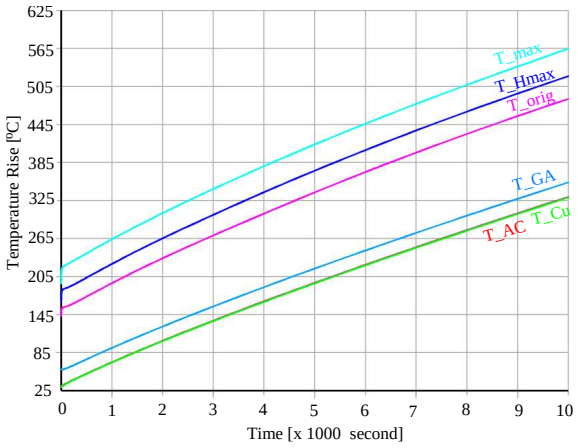

Figure 4: Temperature rise [°C] from static state in first 10000 second at the 6 locations in the water cooling failure.

Table 2: ANSYS calculation results for the beam window

Window Material	Beam Size (mm)	Temperature at center (K) after pulse	before pulse	Maximum Stress at center (MPa) after pulse	before pulse
TESLA Ti 0.5 mm	σ=1	882	362	776	125
	σ=3	414	356	206	117
Be 0.01 inch	σ=1	449	318	442	184
	σ=3	332	315	207	173
Be 0.02 inch	σ=1	448	318	328	82
	σ=3	332	315	113	72

a) Temperature is low enough so that the dump can operate safely in air under normal condition.

b) The dump can afford the water-cooling failure for about 2 hours.

c) In normal operation, the thermal contact won't be degraded because the temperature rise in the graphite core is much larger than that in aluminum. However, in case of a water cooling failure, the thermal contact at the graphite-aluminum interface will be degraded since aluminum has larger thermal expansion rate. Therefore, some measures are needed to ensure the thermal contacting there.

The core should be equipped with thermocouples to control core integrity.

Beam Window

Thermal and stress analyses have been performed for a beam window separating a high vacuum in the beam line from the atmospheric pressure in the beam dump. The nominal parameters for the 3000 bunch operation were considered for two cases of the RMS beam spot size of 1 and 3 mm. MARS15 energy deposition calculations were performed followed by ANSYS analysis. Two designs were investigated for the 5-cm diameter window just upstream of the beam dump. Results are given in Table 2.

First, the TESLA-type configuration was studied with a 0.5-mm titanium window encapsulated in two 10-mm (at center) graphite holders. In the σ=1 mm case, the stress induced by the instant temperature rise is 776 MPa which is beyond the stress limit of 560 MPa, that is yield strength for titanium as given in Table1. The stress for σ=3 mm case is 206 MPa which is below the stress limit. However, our main concern is the significant difference cross the graphite-titanium bonding.

Second, a simple beryllium window was studied. Here we looked at two thicknesses: 0.01 inch and 0.02 inch. The highest temperature is immediately after each beam pulse. The thermal stresses at highest temperature are significant. Total stress is determined by both thermal expansion and atmospheric pressure.

Finally, the simple beryllium window with 0.02-inch thickness is considered to meet the stress required.

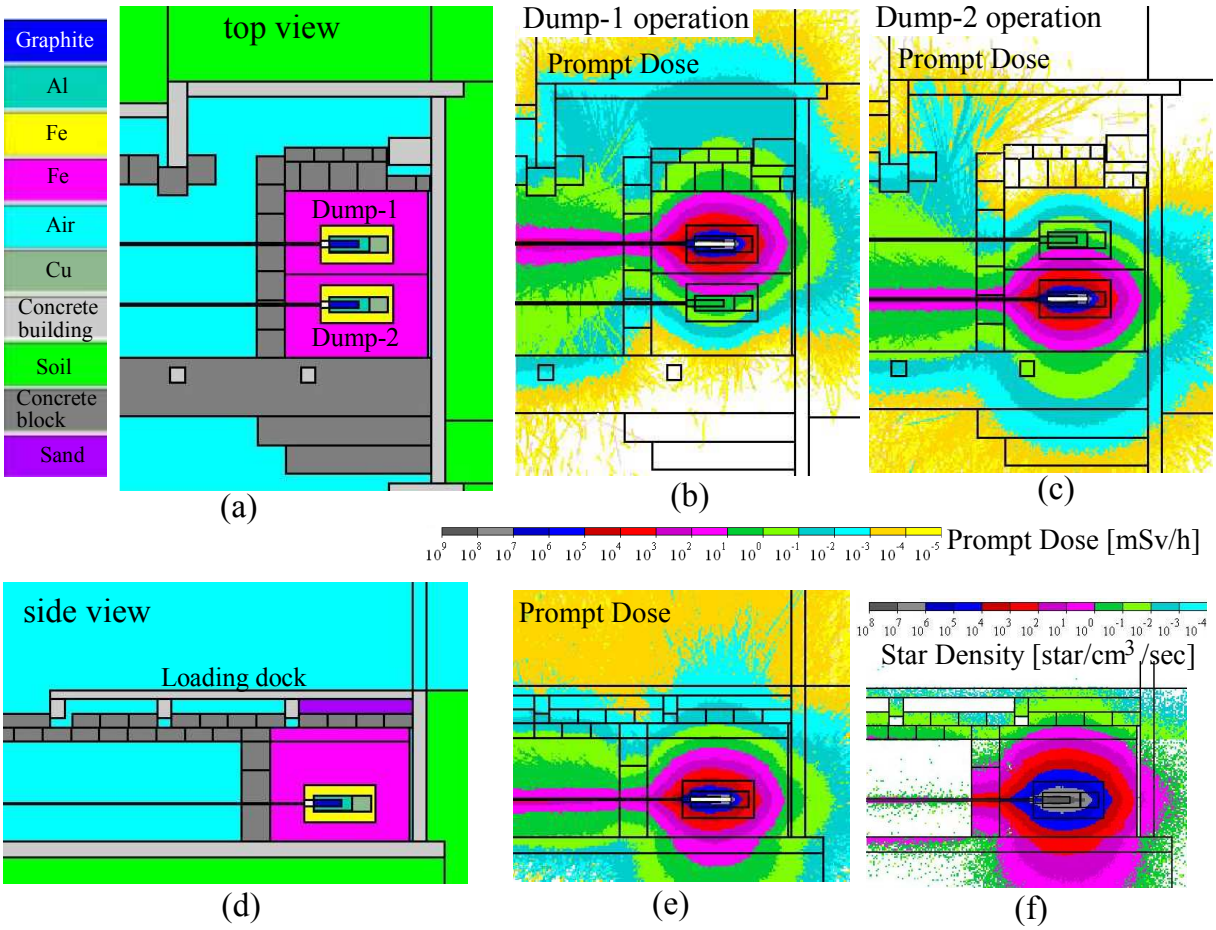

Figure 5: Top views of twin-dump (a)geometry and prompt-dose rate for (b)dump-1 and (c)dump-2 operation, and side views of (d)geometry and (e)prompt-dose rate and (f)star density.

MARS15 SHIELDING SIMULATION

Unlimited occupancy, where the prompt dose rate is below 0.1 mrem/hr (= 1.0 μSv/hr) [3], is assumed in the ILCTA experimental hall. Shielding design around the core-box was optimized in MARS15 calculations to satisfy the design goal. Radiation field outside the bunker is relatively generated by high-energy neutrons (above 20 MeV) in photo-nuclear reactions in the graphite core. High-energy neutrons are most effectively absorbed by a high-Z material. Therefore, the best and cheapest solution is the iron shielding around the core-box, and 3 to 6 feet concrete outside shielding to absorb low-energy neutrons produced through iron.

Fig. 5 shows the optimized shielding design and MARS15 simulation results for a twin beam dump which is currently planned for ILCTA. Maximum beam power is 50 kW for both beam dumps without simultanious operation. Figs. 5(b) and (c) show horizontal distributions of prompt-dose rate for the dump-1 and -2 operations, respectively. Dose rates for both cases are below 0.1 mrem/hr beyond the side-additional concrete wall as shown in figures. Fig. 5(e) shows vertical distribution of prompt-dose rate, and the results for dump-1 and -2 operations are identical. Although dose rate above the loading dock is slightly above 0.1 mrem/hr, personnel access in this area can be controlled during the operation.

Activation of sump water under the hall floor and around the dump shielding can be estimated through star density in soil region. From Figs. 5(b), (c) and (e), prompt dose rate in the soil region under the floor is much higher than those in forward or side soil regions. Therefore, soil activation under the floor can be the most serious. A maximum star density under the floor is about 100 stars/cm^3/sec as shown in Fig. 5(f), and a star density averaged over a dirt volume which contains 99% of stars (as required by a concentration model [3]) is less than 1 star/cm^3/sec. These are well below the 3.4×10^4 and 650 stars/cm^3/sec limits [4], respectively.

REFERENCES

[1] N.V. Mokhov, "The MARS Code System User's Guide", Fermilab-FN-628 (1995); N.V. Mokhov et al, Fermilab-Conf-04/053 (2004); $http://www-ap.fnal.gov/MARS/$.

[2] J. Kidd, N.V. Mokhov, C.T. Murphy, et al, Proc. Part. Acc. Conf., IEEE, vol. 2, p. 2274 (1981).

[3] J.D. Cossairt, Private communication, July 2006.

[4] W.S. Higgins, Private communication, June 2006.